Novel "Multipoint" Molecular Recognition of Nucleobases by a New Zinc(II) Complex of Acridine-Pendant Cyclen (Cyclen = 1,4,7,10-Tetraazacyclododecane)

Mitsuhiko Shionoya,† Takuya Ikeda,† Eiichi Kimura,*,† and Motoo Shiro‡

Contribution from the Department of Medicinal Chemistry, School of Medicine, Hiroshima University, Kasumi 1-2-3, Minami-ku, Hiroshima 734, Japan, and Rigaku Corporation, Matsubaracho 3-9-12, Akishima, Tokyo 196, Japan

Received November 19, 1993®

Abstract: A zinc(II) complex of acridine-pendant cyclen, **4**·2ClO_4 (cyclen = 1,4,7,10-tetraazacyclododecane, **1**), has been designed and synthesized as a new "multipoint" nucleobase receptor molecule in aqueous solution at physiological pH and compared with a Zn^{II} pendantless cyclen complex **2** recently discovered (ref 9) as a highly selective host for dT (deoxythymidine) and U (uridine). The strong acidity of Zn^{II} in **2** is retained in **4**; the water at the fifth coordination site has a pK_a value of 7.46 ± 0.02, L–Zn–OH_2 ⇌ L–Zn–OH^-. Interaction of **4** with a variety of nucleosides has been studied by potentiometric pH titration, ^1H and ^{13}C NMR, IR, UV–vis, and fluorescence spectroscopy. The effects of the acridine functionality in **4** are (i) an enhanced 1:1 association with N(3)-deprotonated dT (log K = 7.2 ± 0.1 at 25 °C and I = 0.10 ($NaNO_3$)) and its congeners, implying an additional acridine–thymine aromatic stacking interaction; (ii) a different interaction mode with dG (2′-deoxyguanosine) (log K = 5.0 ± 0.1 for the N(1)-deprotonated form and 4.1 ± 0.1 for the free form) while no interaction was observed with **2**, but **4** does not interact at all with the nucleosides dA (2′-deoxyadenosine) and dC (2′-deoxycytidine); and (iii) high selectivity for dT among all of the DNA nucleosides in aqueous solution. The strong "multipoint" recognition of **4** with dT is proven by IR, NMR, and the X-ray analyses of an isolated 1:1 ternary complex of **4** with N(3)-deprotonated 1-methylthymine, **10**·ClO_4·$2H_2O$. The X-ray crystal analysis of **10**·ClO_4·$2H_2O$ shows a distorted square-pyramidal N_5-coordinate structure with a strong interaction between the Zn^{II} and the N(3″)-deprotonated anion of the pyrimidine ring (Zn(1)–N(3″) = 1.987(4) Å). The carbonyl oxygen O(2″) of the pyrimidine ring forms a hydrogen bond directly with a cyclen N(10)–H group (O(2″)–N(10) = 2.881(5) Å), while the other O(4″) binds indirectly with a diagonal N(4)–H group via a water molecule. As postulated from the enhanced stability for the **4**–dT complex, a strong cofacial stacking interaction is found between the acridine (at C(1′), C(2′), C(4′), C(4a′), and C(9a′)) and the pyrimidine ring with the plane-to-plane separation ranging from 3.285 to 3.419 Å. Crystals of **10**·ClO_4·$2H_2O$ ($C_{28}H_{40}N_7O_8Cl_1Zn_1$) are C-centered monoclinic, space group $C2/c$ (#15) with a = 15.312(3) Å, b = 21.920(3) Å, c = 18.774(2) Å, β = 101.68 (1)°, V = 6171 (1) Å^3, and Z = 8. Full-matrix least-squares refinement converged at R = 0.062 and R_w = 0.093 for 3573 independent reflections. A ternary complex **11** composed of **4** and the free form of dG was isolated by mixing **4** and dG in CH_3CN–H_2O. The X-ray crystal analysis of **11**·2BF_4·2.5H_2O shows a distorted square-pyramidal N_5-coordinate structure containing the fifth coordination from N(7″) of the dG purine ring to Zn^{II} (Zn(1)–N(7″) = 2.04(1) Å). The carbonyl oxygen O(6″) of the purine ring forms a hydrogen bond with a cyclen N(4)–H group (O(6″)–N(4), 3.01 (1) Å). A strong cofacial stacking interaction between the acridine (at C(1′), C(2′), C(3′), C(4′), and C(4a′)) and the purine ring greatly helps to stabilize the complex. Crystals of **11**·2BF_4·2.5H_2O ($C_{32}H_{47}N_{10}O_{6.5}B_2F_8Zn_1$) are monoclinic, space group $P2_1$ (#4) with a = 10.892(4) Å, b = 21.230(2) Å, c = 17.465(2) Å, β = 101.19(1)°, V = 3974(1) Å^3, and Z = 4. Full-matrix least-squares refinement converged at R = 0.083 and R_w = 0.104 for 4473 independent reflections.

Introduction

Molecular recognition of DNA, RNA, and related biomolecules has currently been attracting great interest.[1-7] Of all the approaches, the recognition of a specific nucleobase and a specific sequence in a nucleic acid polymer is the most challenging. Receptor molecules for specific nucleic acid constituents can be applied to antisense drugs,[8] which have recently been proposed as a new class of antiviral and anticancer pharmaceuticals. In

† Hiroshima University.
‡ Rigaku Corp.
® Abstract published in *Advance ACS Abstracts,* March 15, 1994.

(1) (a) Kimura, E.; Kodama, M.; Yatsunami, T. *J. Am. Chem. Soc.* **1982**, *104*, 3182. (b) Kimura, E. *Top. Curr. Chem.* **1985**, *128*, 131, 141. (c) Umezawa, Y.; Kodama, M.; Takami, W.; Kimura, E.; Koike, T.; Nada, H. *Anal. Chem.* **1988**, *60*, 2392. (d) Kimura, E.; Kuramoto, Y.; Koike, T.; Fujioka, H.; Kodama, M. *J. Org. Chem.* **1990**, *55*, 42.

(2) (a) Hosseini, M. W.; Blacker, A. J.; Lehn, J.-M. *J. Am. Chem. Soc.* **1990**, *112*, 3896 and references cited therein. (b) Lehn, J.-M.; Mascal, M.; DeCian, A.; Fischer, J. *J. Chem. Soc., Chem. Commun.* **1990**, 479.

(3) (a) Muehldolf, A. V.; Engen, D. V.; Warner, J. C.; Hamilton, A. D. *J. Am. Chem. Soc.* **1988**, *110*, 6561. (b) Goswami, S.; Hamilton, A. D.; Van Engen, D. *J. Am. Chem. Soc.* **1989**, *111*, 3425 and references cited therein. (c) Hamilton, A. D.; Little, D. *J. Chem. Soc., Chem. Commun.* **1990**, 297. (d) Hamilton, A. D. In *Bioorganic Chemistry Frontiers*; Dugas, H., Ed.; Springer-Verlag: Berlin, Heidelberg, 1991; Vol. 2, pp 115–174.

(4) (a) Rebek, J., Jr. *Angew. Chem., Int. Ed. Engl.* **1990**, *29*, 245. (b) Park, T. K.; Schroeder, J.; Rebek, J., Jr. *Tetrahedron* **1991**, *47*, 2507. (c) Rotello, V. M.; Viani, E. A.; Deslongchamps, G.; Murray, B. A.; Rebek, J., Jr. *J. Am. Chem. Soc.* **1993**, *115*, 797. (d) Conn, M. M.; Deslongchamps, G.; de Mendoza, J.; Rebek, J., Jr. *J. Am. Chem. Soc.* **1993**, *115*, 3548 and references cited therein.

(5) (a) Furuta, H.; Magda, D.; Sessler, J. L. *J. Am. Chem. Soc.* **1991**, *113*, 978. (b) Kral, U.; Sessler, J. L.; Furuta, H. *J. Am. Chem. Soc.* **1992**, *114*, 8704.

(6) (a) Ebmeyer, F.; Vögtle, F. *Angew. Chem., Int. Ed. Engl.* **1989**, *28*, 7. (b) Aoyama, Y.; Tanaka, Y.; Sugahara, S. *J. Am. Chem. Soc.* **1989**, *111*, 5397. (c) Zimmerman, S.; Weiming, W. *J. Am. Chem. Soc.* **1989**, *111*, 8054. (d) Adrian, J. C., Jr.; Wilcox, C. S. *J. Am. Chem. Soc.* **1989**, *111*, 8055. (e) Slavin, L. L.; Bose, R. N. *J. Chem. Soc., Chem. Commun.* **1990**, 1256. (f) Schneider, H.-J.; Blatter, T.; Palm, B.; Pflingstag, U.; Rudiger, V.; Theis, I. *J. Am. Chem. Soc.* **1992**, *114*, 7704.

(7) For recent reviews and articles on interactions of metal ions or complexes with nucleic acid constituents, see: (a) Reedijk, J. *Pure Appl. Chem.* **1987**, *59*, 181. (b) Kalbitzer, H. R. *Met. Ions Biol. Syst.* **1987**, *22*, 81. (c) Lippert, B. *Prog. Inorg. Chem.* **1989**, *37*, 1. (d) Sundquist, W. I.; Lippard, S. *J. Coord. Chem. Rev.* **1990**, *100*, 293. (e) Pyle, A. H.; Barton, J. K. *Prog. Inorg. Chem.* **1990**, *38*, 413. (f) Lin, M.; Lee, M.; Yue, K. T.; Marzilli, L. G. *Inorg. Chem.* **1993**, *32*, 3217. (g) Krotz, A. H.; Kuo, L. Y.; Shields, T. P.; Barton, J. K. *J. Am. Chem. Soc.* **1993**, *115*, 3877. (h) Krizanovic, O.; Sabat, M.; Beyerle-Pfnur, R.; Lippert, B. *J. Am. Chem. Soc.* **1993**, *115*, 5538. (i) Kickham, J. E.; Loeb, S. J.; Murphy, S. L. *J. Am. Chem. Soc.* **1993**, *115*, 7031. (j) Sigel, H. *Chem. Soc. Rev.* **1993**, *22*, 255.

0002-7863/94/1516-3848$04.50/0

Chart 1

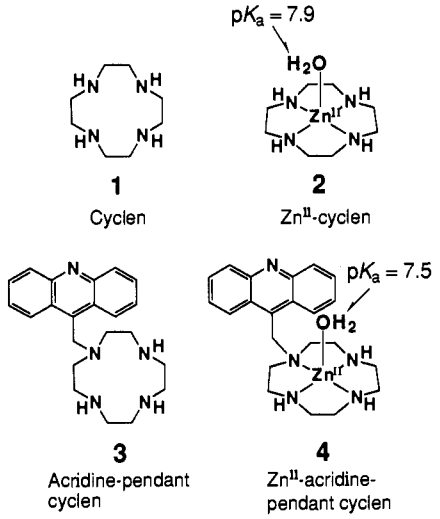

the process of DNA or RNA recognition, structural and electronic information of the nucleobases is transferred to and stored within the receptor molecules. An appropriate combination of intermolecular binding modes (metal coordination, hydrogen bonding, hydrophobic and electrostatic interactions, etc.) is required for enhanced discrimination in order to make an artificial receptor molecule that recognizes and binds to specific sites of nucleic acid polymers.

Recently,[9] we discovered that Zn^{II}–cyclen complex **2** (cyclen = 1,4,7,10-tetraazacyclododecane, **1** in Chart 1) is a highly selective host for dT (deoxythymidine) and U (uridine) among all of the nucleosides in aqueous solution. The original idea came from our discovery of the outstanding Lewis acid properties of a zinc(II) complex with the macrocyclic triamine, [12]aneN$_3$ (1,5,9-triazacyclododecane), which tends to bind at the vacant fourth coordination site with anionic ligands rather than with neutral nitrogen donors.[10] Thus, unlike other transition metal complexes, there is little interaction between the Zn^{II} complex **2** and the donor sites of nucleobases dG (2′-deoxyguanosine) (–NH$_2$ at C(2), O(6), and N(7)), dA (2′-deoxyadenosine) (–NH$_2$ at C(2) and N(7)), and dC (2′-deoxycytidine) (O(2) and –NH$_2$ at C(4)).[9] By contrast, the guests dT and U both contain an "imide" –CONHCO– moiety, which sets then them apart from the other nucleosides (Chart 2). In the resulting complexes **5** (Scheme 1), the "imide" proton dissociates (pK_a = 9.8 for dT and 9.2 for U at 25 °C and I = 0.10 (NaClO$_4$)) to be replaced by Zn^{II}, and both adjacent carbonyl oxygens hydrogen bond directly and/or indirectly via a water molecule with the cyclen NH groups at the complementary positions.[9] The significance of the "imide" functionality can be illustrated by the following facts: (i) if it is replaced by an "amide" (e.g. Ino (inosine)), the 1:1 complexation constant (log K = 4.2) is smaller than that for dT (log K = 5.6) and than that predicted from the "amide" pK_a value of 8.8, and (ii) if one of the carbonyls is replaced by an amino group (e.g. dG), no interaction occurs at all, even though dG possesses a dissociable NH proton (pK_a = 9.4) at the "amide" moiety. It was thus concluded that a "three-point" recognition process (Zn^{II}–N- interaction and two hydrogen bonds) was operating. The notion of this novel "three-point" recognition was proven by the X-ray

Chart 2

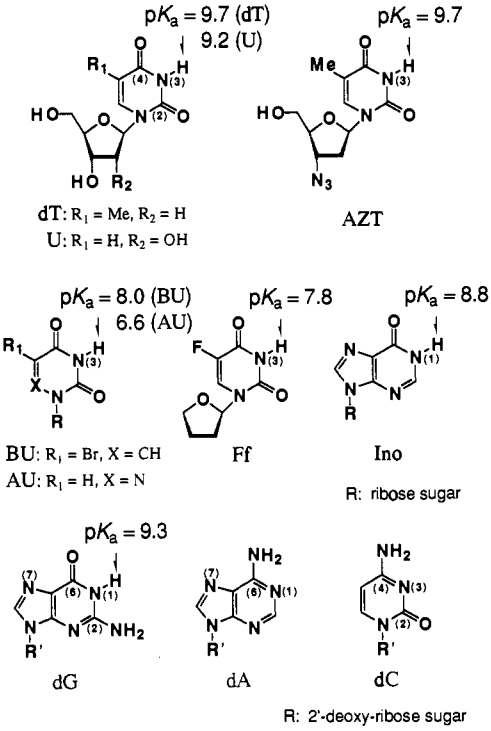

Scheme 1

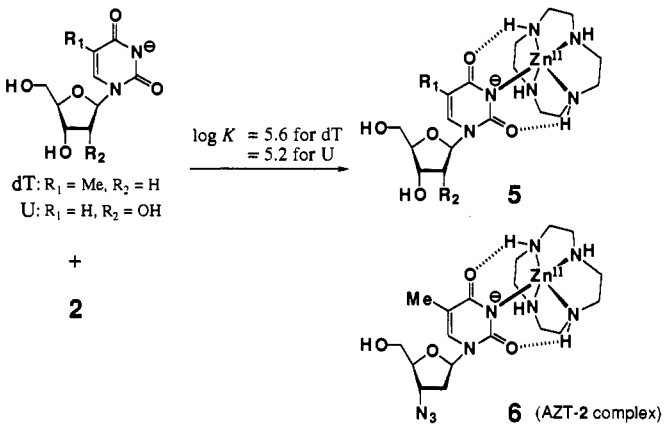

crystal structure of a ternary complex **6** composed of AZT (3′-azido-3′-deoxythymidine) and **2**.[9] Most remarkably, these interactions occur even *in aqueous media* where hydrogen bonds cannot normally be sustained. The novel AZT complex **6** remains stable in aqueous solution at physiological pH. Molecular recognition seen in naturally-occurring dA–dT or dG–dC base pairs occurs only in the hydrophobic domain of DNA polymers or in nonaqueous systems.

To further exploit this novel phenomenon of the nucleoside recognition in aqueous solution at physiological pH, the macrocyclic polyamine receptor molecules may be equipped with additional ligands, capable of interacting with nucleobase and/or sugar moieties. In the present study, we have introduced an acridine moiety onto the cyclen ring in anticipation of a step forward to a more efficient "multipoint" recognition. It was hoped that the aromatic acridine ring would produce an additional "stacking interaction" with the nucleobases, whereby an even stronger interaction might occur in aqueous solution at physiological pH. Moreover, such a stacking agent might initially insert into the DNA or RNA strand to allow the subsequent interaction of the Zn^{II}–cyclen moiety with a thymine (or uracil) base and/or phosphoester anions. It has been previously shown that the Zn^{II}–cyclen complex **2** can interact with phosphomo-

(8) (a) Uhlmann, E.; Peyman, A. *Chem. Rev.* **1990**, *90*, 543. (b) Milligan, J. F.; Matteucci, M. D.; Martin, J. C. *J. Med. Chem.* **1993**, *36*, 1923 and references cited therein.

(9) Shionoya, M.; Kimura, E.; Shiro, M. *J. Am. Chem. Soc.* **1993**, *115*, 6730.

(10) (a) Kimura, E.; Shiota, T.; Koike, T.; Shiro, M.; Kodama, M. *J. Am. Chem. Soc.* **1990**, *112*, 5805. (b) Koike, T.; Kimura, E.; Nakamura, I.; Hashimoto, Y.; Shiro, M. *J. Am. Chem. Soc.* **1992**, *114*, 7338. (c) Kimura, E.; Shionoya, M.; Hoshino, A.; Ikeda, T.; Yamada, Y. *J. Am. Chem. Soc.* **1992**, *114*, 10134.

noesters (e.g. log K = 3.3 with p-nitrophenyl phosphate)[11] or hydrolyze monoanionic phosphodiesters.[12]

Herein, we present the synthesis of the new ligand, acridine-pendant cyclen **3**, and its Zn^{II} complex **4**, as well as its novel interaction mode with nucleosides.

Experimental Section

General Information. All reagents and solvents used were of analytical grade. dT (deoxythymidine), dG (2′-deoxyguanosine), dC (2′-deoxycytidine), dA (2′-deoxyadenosine), U (uridine), Ff (ftorafur, 5-fluoro-1-(tetrahydro-2-furyl)uracil), AZT (3′-azido-3′-deoxythymidine), Ino (inosine), BU (5-bromouridine), AU (6-azauridine), and 1-methylthymine were all purchased from Sigma Chemical Co. Ltd. Cyclen as a tetrahydrochloride salt was purchased from Tokyo Kasei Co. Ltd. Anhydrous CH_3CN, distilled from calcium hydride, was used for the synthesis of **3**. 9-(Bromomethyl)acridine (**7**), was prepared from iminostilbene in two steps according to the literature.[13] IR spectra were recorded on a Shimadzu FTIR-4200 spectrophotometer.

Synthesis of Acridine-Pendant Cyclen 3. To a solution of cyclen (**1**, 1.42 g, 8.3 mmol) in 40 mL of anhydrous hot CH_3CN was slowly added a solution of 9-(bromomethyl)acridine (**7**, 1.12 g, 4.1 mmol) in 100 mL of anhydrous CH_3CN. The reaction mixture was stirred at room temperature for 12 h. After the removal of the solvent under diminished pressure, the residue was dissolved in 0.2 M HCl aqueous solution. The aqueous solution was washed with several portions of CH_2Cl_2. After addition of 5 M NaOH aqueous solution, the alkaline solution was extracted with several portions of CH_2Cl_2. The combined organic layer was dried over anhydrous Na_2CO_3 and then concentrated. The crude oil was taken up in C_2H_5OH and acidified with concentrated HCl to precipitate the desired hydrochloride salt of **3**. This procedure was repeated once more to obtain pure **3**·4HCl·4H_2O (1.50 g, yield 62%). Mp 110 °C (dec). IR (KBr): 3430, 2918, 2766, 2457, 2390, 1634, 1586, 1468, 1441, 1427, 1399, 1366, 760 cm^{-1}. ^1H NMR (D_2O, 20 mM, pD 3): δ 2.92–3.32 (16H, brm, CH_2N), 5.09 (2H, s, $ArCH_2$), 8.06 (2H, ddd, J = 8.8, 6.8, 1.1 Hz, aromatic), 8.33 (2H, ddd, J = 8.8, 6.8, 1.1 Hz, aromatic), 8.41 (2H, brd, aromatic), 8.69 (2H, brd, aromatic). ^{13}C NMR (D_2O, 20 mM, pD 3): δ 44.5, 44.9, 47.1, 52.4, 52.6, 123.7, 128.1, 129.1, 132.1, 140.5, 142.3, 156.7. Anal. Calcd for $C_{22}H_{29}N_5$·4HCl·4H_2O: C, 45.45; H, 7.11; N, 12.05. Found: C, 45.36; H, 7.02; N, 12.18.

Synthesis of Acridine-Pendant Zn^{II}–Cyclen Complex 4·2ClO_4. To a solution of the free form of **3** in 30 mL of C_2H_5OH, prepared from **3**·4HCl·4H_2O (450 mg, 0.77 mmol) by treatment with base and then extraction, was slowly added a solution of $Zn^{II}(ClO_4)_2$·6H_2O (288 mg, 0.77 mmol) in 9 mL of C_2H_5OH at 40–50 °C with stirring. Yellowish prisms of **4**·2ClO_4 (469 mg, yield 94%) were obtained by recrystallization from CH_3CN–H_2O. IR (KBr): 3437, 3293, 2930, 2883, 1559, 1522, 1456, 1360, 1285, 1180, 1144, 1090, 974, 770, 716, 627 cm^{-1}. ^1H NMR (CD_3CN, 20 mM): δ 2.53–2.80 (8H, m, CH_2N), 2.85–2.98 (6H, m, CH_2N), 3.13 (1H, brt, NH), 3.21–3.30 (2H, m, CH_2N), 3.55 (2H, brt, NH), 5.03 (2H, s, $ArCH_2$), 7.76 (2H, ddd, J = 9.0, 6.6, 1.3 Hz, aromatic), 7.99 (2H, ddd, J = 8.7, 6.6, 1.2 Hz, aromatic), 8.25 (2H, brd, J = 9.0 Hz, aromatic), 8.40 (2H, brd, J = 8.7 Hz, aromatic). ^{13}C NMR (CD_3CN, 20 mM): δ 43.8, 44.7, 45.9, 48.4, 52.1, 125.5, 127.7, 128.3, 131.3, 131.6, 137.0, 149.8. Anal. Calcd for $C_{22}H_{29}N_5Zn_1$·2ClO_4·H_2O: C, 40.92; H, 4.84; N, 10.84. Found: C, 40.94; H, 4.98; N, 10.65.

Synthesis of N(3)-Deprotonated 1-Methylthymine–(Acridine-Pendant Zn^{II}–Cyclen) Complex 10·ClO_4·2H_2O. To a solution of 1-methylthymine (28 mg, 0.2 mmol) in 4 mL of 0.05 M NaOH aqueous solution was added a solution of **4**·2ClO_4 (129 mg, 0.2 mmol) in 6 mL of hot CH_3CN. The reaction mixture was heated at 40–50 °C for 10 min. After the mixture was cooled, 1 mL of 1 M $NaClO_4$ aqueous solution was added to the mixture, which was allowed to stand in a desiccator in the presence of KOH under diminished pressure. The resulting pale yellow prisms were recrystallized from CH_3OH–H_2O (106 mg, yield 75%) and then subjected to X-ray analysis. IR (KBr): 1661, (C=O), 1626 (C=O), 1564 (C=C), 1547 (C=C), 1146, 1107, 1090 (ClO_4^-) cm^{-1}. ^1H NMR (CD_3OD, 20 mM): δ 1.77 (3H, m, 5-CH_3), 2.69–3.05 (14H, m, NCH_2), 3.14 (3H, d, J = 2.7 Hz, NCH_3), 3.34 (2H, brs, NCH_2), 3.52 (1H, br, NH), 4.06 (2H, br, NH), 5.00 (2H, d, J = 2.5 Hz, $ArCH_2$), 7.09 (1H, brs, vinylic proton), 7.64 (2H, m, aromatic), 7.79 (2H, m, aromatic), 8.13 (2H, dd, J = 8.3, 2.2 Hz, aromatic), 8.42 (2H, d, J = 6.9 Hz, aromatic). ^{13}C NMR (CD_3OD, 20 mM): δ 13.1, 36.5, 44.5, 44.9, 46.6, 52.8, 97.3, 110.8, 126.0, 127.7, 128.3, 130.3, 131.5, 139.8, 149.5, 158.9, 174.3 (the benzylic carbon signal seems to be concealed behind that of CD_3OD). Anal. Calcd for $C_{28}H_{36}N_7O_2Zn_1$·ClO_4·2H_2O: C, 47.80; H, 5.73; N, 13.94. Found: C, 47.90; H, 5.57; N, 13.94.

Synthesis of dG–(Acridine-Pendant Zn^{II}–Cyclen) Complex 11·2BF_4·2.5H_2O. To a solution of dG (22 mg, 0.075 mmol) in 4 mL of H_2O was added a solution of **4**·2ClO_4 (48 mg, 0.075 mmol) in 4 mL of hot CH_3CN. A solution of $NaBF_4$ (110 mg) in 2 mL of H_2O, adjusted at pH ~ 7, was added to the mixture, which was allowed to stand in a desiccator in the presence of KOH under diminished pressure. Orange prisms, suitable for X-ray analysis, were obtained (57 mg, yield 81%). IR (KBr): 1694 (C=O), 1636, 1597, 1084, 1034 (BF_4^- for the last two) cm^{-1}. ^1H NMR (dimethyl sulfoxide-d_6, 17 mM): δ 2.34–2.52 (2H, m, 2‴-H), 2.62–3.02 (14H, m, NCH_2), 3.2–3.3 (2H, m, NCH_2), 3.53 (2H, m, 5‴-H), 3.85–3.88 (1H, m, 4‴-H; 1H, br, cyclen-NH), 4.38 (1H, m, 3‴-H), 4.7–4.8 (2H, br, cyclen-NHs), 4.91 (1H, t, J = 5.5 Hz, 5‴-OH), 4.96 (2H, brs, $ArCH_2$), 5.36 (1H, d, J = 4.2 Hz, 3‴-OH), 6.07 (1H, pseudo-t, J = 6.8/6.6 Hz, 1‴-H), 6.79 (2H, brs, 2″-NH_2), 7.53 (2H, t, J = 7.5 Hz, aromatic), 7.74 (2H, pseudo-t, J = 8.2/6.8 Hz, aromatic), 7.84 (1H, s, 8″-H), 8.09 (2H, d, J = 8.4 Hz, aromatic), 8.37 (2H, d, J = 8.8 Hz, aromatic), 10.82 (1H, s, amide) (for the numbering, see Scheme 7). ^{13}C NMR (dimethyl sulfoxide-d_6, 17 mM): δ 38.88, 42.32, 42.46, 42.87, 42.95, 44.55, 44.66, 47.70, 51.31, 51.38, 61.21, 70.13, 83.09, 87.84, 113.81, 124.59, 126.09, 126.25, 129.57, 129.62, 136.77, 136.92 (C8″), 147.97, 149.95, 154.08, 155.58. Anal. Calcd for $C_{32}H_{42}N_{10}O_4Zn_1$·2$BF_4$·2.5$H_2O$: C, 42.02; H, 5.18; N, 15.31. Found: C, 41.83; H, 5.17; N, 15.14.

Potentiometric pH Titrations. The preparation of the test solutions and the calibration of the electrode system (Orion Research Expandable Ion Analyzer EA920 and Orion Research Ross Combination pH Electrode 81028N) were described earlier.[14] All samples were kept under an argon (>99.999% purity) atmosphere. The solution temperature was maintained at 25.0 ± 0.1 °C, and the ionic strength was adjusted to 0.10 M with $NaNO_3$. For the determination of log K_n ($K_n = [H_nL]/([H_{n-1}L]a_{H^+})$) values, at least two independent titrations were carried out. The calculation methods for protonation constants (log K_n) of the ligand and metal complexation constants are the same as described previously.[15,16] Figure 1 shows pH titration curves for $[3{\cdot}5H^+]^{5+}$ in the absence and the presence of an equimolar amount of Zn^{II} at 25 °C and I = 0.10 ($NaNO_3$).

The deprotonation constants pK_a for nucleosides were calculated by the method previously described.[15] The values of K_w (= $[H^+][OH^-]$), f_{H^+}, and f_{OH^-} used in the computation were $10^{-13.79}$, 0.83, and 0.76, respectively.

Measurement of the complexation constants, K(ZnL–S) (= [ZnL–S]/([ZnL][S]), M^{-1}), for a variety of nucleosides was conducted by a potentiometric pH titration method at 25 °C and I = 0.10 ($NaNO_3$). Aqueous solutions (50 mL) of acridine-pendant Zn^{II}–cyclen complex ([**4**] = 1.0 mM) with (or without) substrates ([HS] = 1.0 mM) were titrated with carbonate-free 0.100 M NaOH aqueous solution. HS and S represent a nucleoside in a free form and an N(3)– (or N(1)– for Ino and dG) deprotonated anionic form, respectively. Typical titration data for dT and **4**·2ClO_4 with and without dT are plotted in Figure 2.

The calculation method for the complexation constants with dT and its homologues was described earlier.[9] Complexation constant K(ZnL–S) values are obtained from pH and a values at each titration point ($0 < a < 2$). a is the number of equivalents of base added.

Measurement of the complexation constants, K(ZnL–HS) (= [ZnL–HS]/([ZnL][HS]), M^{-1}) and K(ZnL–S), for dG was also conducted by a potentiometric pH titration method at 25 °C and I = 0.10 ($NaNO_3$). pH Titration data for dG and **4** with and without dG are plotted in Figure 8. The following equilibria and equations were considered to take place in the buffer region ($0 < a < 2$).

(11) Koike, T.; Kimura, E. Unpublished results.

(12) (a) Koike, T.; Kimura, E. *J. Am. Chem. Soc.* **1991**, *113*, 8935. (b) Shelton, V. H.; Morrow, J. R. *Inorg. Chem.* **1991**, *30*, 4295.

(13) (a) Schindler, H.; Blattner, H. *Helv. Chem. Acta* **1961**, *44*, 753. (b) Rumpf, P.; Reynaud, R. *Bull. Soc. Chim. Fr.* **1962**, 2241. (c) Akasaka, K.; Suzuki, T.; Ohrui, H.; Meguro, J.; Shindo, Y.; Takahashi, H. *Anal. Lett.* **1987**, *20*, 1581.

(14) Kimura, E.; Koike, T.; Uenishi, K.; Hedigar, M.; Kuramoto, M.; Joko, S.; Arai, Y.; Kodama, M.; Iitaka, Y. *Inorg. Chem.* **1987**, *26*, 2975.

(15) Kimura, E.; Koike, T.; Shiota, T.; Iitaka, Y. *Inorg. Chem.* **1990**, *29*, 4621.

(16) Kimura, E.; Yamaoka, M.; Morioka, M.; Koike, T. *Inorg. Chem.* **1986**, *25*, 3883.

$$ZnL + H_2O \rightleftharpoons ZnL(OH^-) + H^+;\ K_{OH} = [ZnL(OH^-)]a_{H+}/[ZnL] \quad (1)$$

$$ZnL + S \rightleftharpoons ZnL\text{–}S;\ K(ZnL\text{–}S) = [ZnL\text{–}S]/([ZnL][S]) \quad (2)$$

$$ZnL + HS \rightleftharpoons ZnL\text{–}HS;\ K(ZnL\text{–}HS) = [ZnL\text{–}HS]/([ZnL][HS]) \quad (3)$$

$$ZnL\text{–}HS \rightleftharpoons ZnL\text{–}S + H^+;\ K_{TC} = [ZnL\text{–}S]a_{H+}/([ZnL\text{–}HS]) \quad (4)$$

Substrate mass balance:

$$C_{S(total)} = [HS] + [S] + [ZnL\text{–}S] + [ZnL\text{–}HS] \quad (5)$$

Metal mass balance:

$$C_{ZnL(total)} = [ZnL] + [ZnL(OH^-)] + [ZnL\text{–}S] + [ZnL\text{–}HS] \quad (6)$$

Proton mass balance:

$$C_\alpha = aC_{ZnL(total)} + [H^+] - [OH^-] = [ZnL\text{–}S] + [ZnL(OH^-)] + [S] \quad (7)$$

From the above equations, the following equations are derived.

$$C_{S(total)} = \delta[ZnL\text{–}S] + \beta[S] \quad (8)$$

$$C_{ZnL(total)} = \delta[ZnL\text{–}S] + (1 + \gamma)[ZnL] \quad (9)$$

$$C_\alpha = [ZnL\text{–}S] + \gamma[ZnL] + [S] \quad (10)$$

where $\beta = ([HS] + [S])/[S]$, $\gamma = K_{OH}/a_{H+}$, and $\delta = ([ZnL\text{–}HS] + [ZnL\text{–}S])/[ZnL\text{–}S]$. From the eqs 8–10, one can derive the following equations.

$$[S] = (C_{S(total)} - \delta[ZnL\text{–}S])/\beta \quad (11)$$

$$[ZnL] = (C_{ZnL(total)} - \delta[ZnL\text{–}S])/(1 + \gamma) \quad (12)$$

$$[ZnL\text{–}S] = [\beta\gamma C_{ZnL(total)} + (1 + \gamma)(C_S - \beta C_\alpha)]/[(1 + \gamma)(\delta - \beta) + \beta\gamma\delta] \quad (13)$$

$$K(ZnL\text{–}HS) = K_{OH}K(ZnL\text{–}S)/K_{TC} \quad (14)$$

The complexation constants K(ZnL–HS) and K(ZnL–S) were obtained from an imaginary deprotonation constant (K_{TC}) for the ternary complex of **4** with the free form of dG and pH and α values at each titration point ($0 < a < 2$) by using the eqs 11–14. In the computation, an imaginary K_{TC} value of $10^{-8.42}$ was used as the optimum for the determination of log K(ZnL–S) = 5.0 ± 0.1 and log K(ZnL–HS) = 4.1 ± 0.1.

NMR Studies. ^1H (400 MHz) and ^{13}C NMR (100 MHz) spectra were recorded on a JEOL JNM α400 or JEOL GX400 spectrometer. The chemical shifts are given in ppm with respect to 3-(trimethylsilyl)-propionic-*2,2,3,3-d*$_4$ acid sodium salt (Merck) in D_2O and tetramethylsilane (Merck) in organic solvent as internal standards. For NMR studies of dT in the presence of **4**, solutions of **4**·2ClO_4 (5 mM), dT (5 mM), and a mixture of the two (each 5 mM) were made up in D_2O (99.9 atom % D from Aldrich) and the pD was adjusted by NaOD (Merck). The pD value was corrected for a deuterium isotope effect using pD = [pH meter reading + 0.40].[17]

Crystallographic Studies. A pale yellow prismatic crystal of **10**·ClO_4·2H_2O with dimensions 0.40 × 0.20 × 0.10 mm was used for data collection. The lattice parameters and intensity data were measured on a Rigaku AFC7R diffractometer with graphite monochromated Cu Kα radiation and a 12-kW rotating anode generator. The structure was solved by direct methods, and the non-hydrogen atoms were refined anisotropically. The final cycle of full-matrix least-squares refinement was based on 3573 observed reflections to give $R = 0.062$ and $R_w = 0.093$. All calculations were performed using a TEXSAN crystallographic software package developed by Molecular Structure Corp. (1985). An ORTEP drawing (50% probability ellipsoids) of **10**·ClO_4·2H_2O, with the atom-numbering system, is presented in Figure 6. Figure 7 shows a lattice picture of **10**·ClO_4·2H_2O drawn down the *b* crystallographic direction. Crystallographic parameters, selected bond distances (Å), interligand bond distances (Å), and bond angles (deg) of **10**·ClO_4·2H_2O are listed in Tables 4 and 5, respectively.

An orange prismatic crystal of **11**·2BF_4·2.5H_2O with dimensions 0.30 × 0.25 × 0.10 mm was used for data collection. The final cycle of full-matrix least-squares refinement was based on 4473 observed reflections to give $R = 0.83$ and $R_w = 0.104$. An ORTEP drawing (30% probability ellipsoids) of **11**·2BF_4·2.5H_2O, with the atom-numbering system, is presented in Figure 9. Crystallographic parameters, selected bond distances (Å), interligand bond distances, (Å), and bond angles (deg) of **11**·2BF_4·2.5H_2O are listed in Tables 6 and 7, respectively.

The linear absorption coefficients μ, for Cu Kα radiation are 24.3 and 17.1 cm^{-1} for **10**·ClO_4·2H_2O and **11**·2BF_4·2.5H_2O, respectively. An empirical absorption correction using the program DIFABS[18] was applied which resulted in transmission factors ranging from 0.82 to 1.20 and from 0.78 to 1.18 for **10**·ClO_4·2H_2O and **11**·2BF_4·2.5H_2O, respectively. The data were corrected for Lorentz and polarization effects.

Fluorescence Studies. UV–vis spectra were recorded on a Hitachi U-3200 spectrophotometer and emission spectra on a Shimadzu RF-5000 spectrofluometer interfaced with a DR-15 digital recorder. The solutions (3.4 mL in a 10-mm quartz fluorescence cell) containing 10 μM **4**·2ClO_4 and 10 μM respective nucleoside (dT, Ino, dG, dA, and dC) in HEPES (2-[4-(2-hydroxyethyl)-1-piperazinyl]ethanesulfonic acid) buffer (10 mM, pH 7.6, $I = 0.10$ ($NaNO_3$)) were degassed with argon and kept at 25 °C. Fluorescence spectra of **4** excited at 361 nm in the absence and the presence of each nucleoside are shown in Figure 10. Table 8 summarizes the relative fluorescence intensities of **3** and **4** with and without the nucleosides.

Scheme 2

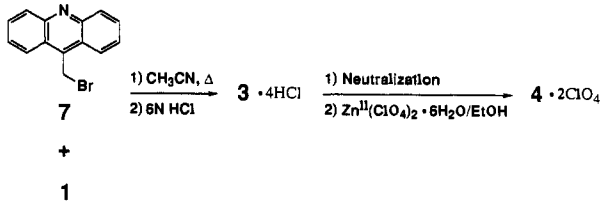

Results and Discussion

Synthesis and Protonation Constants of 3. Acridine-pendant cyclen **3** was synthesized by the reaction of 9-(bromomethyl)-acridine (**7**) with 2 equiv of cyclen in anhydrous CH_3CN (Scheme 2). The free form of **3** obtained as a pale yellow oil was purified as **3**·4HCl·4H_2O by precipitation from C_2H_5OH with concentrated HCl. Characterization of the compound was accomplished using ^1H and ^{13}C NMR, and elemental analysis (C, H, N). This general synthetic route is applicable to the synthesis of homologues with differing side-arm lengths, as well as to the introduction of other intercalating agents, which will be reported later.

The protonation constants (log K_n) of acridine-pendant cyclen **3** were determined by potentiometric pH titration at 25 °C and $I = 0.10$ ($NaNO_3$) (Figure 1a).[19] The protonation constants K_1–K_5 as logarithmic values are assigned in Table 1 and are compared with the K_n values for unsubstituted cyclen (**1**).[20] The protonation constant of the acridine nitrogen in **3** was found to be log $K = 4.4 \pm 0.1$ from the UV–vis absorption changes at 362

(17) Glasoe, P. K.; Long, F. A. *J. Phys. Chem.* **1960**, *64*, 188.

(18) DIFABS: Walker, N.; Stuart. *Acta Crystallogr.* **1983**, *A39*, 158 (an empirical absorption correction program).

(19) Self-association is a well-known phenomenon for aromatic compounds and must therefore be considered in any measurement designed for quantification of monomeric species. Helene et al. proposed several mathematical models derived from simple assumptions to account for ^1H NMR data of self-associating systems (Dimicoli, J.-L.; Helene, C. *J. Am. Chem. Soc.* **1973**, *95*, 1036). From changes in the proton chemical shifts of **4** in aqueous solution at different concentrations, the logarithmic value of association constant K was calculated to be 2.6 ± 0.2 M^{-1} ($K = [A_n]/([A_{n-1}][A])$, M^{-1}). It has been assumed throughout this work that both **3** and **4** behave as monomeric species.

(20) Kodama, M.; Kimura, E. *J. Chem. Soc., Dalton Trans.* **1977**, 2269.

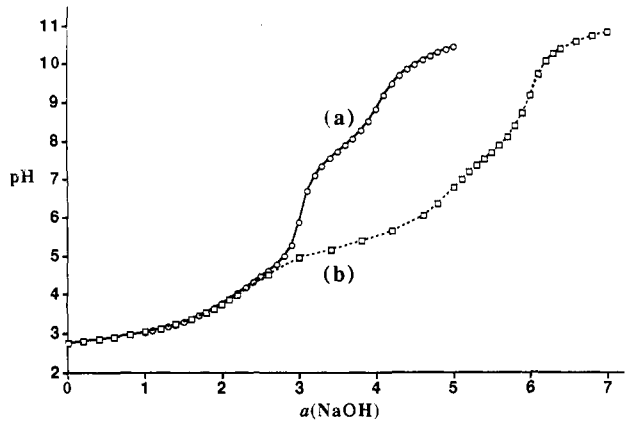

Figure 1. pH Titration data for acridine-pendant cyclen **3** at 25 °C and $I = 0.10$ ($NaNO_3$): (a) 1.0 mM $[3{\cdot}5H^+]^{5+}$; (b) part a + 1.0 mM Zn^{II}. a is the number of equivalents of base added. The data for a and b at $0 < a < 1$ are identical.

Table 1. Protonation Constants K_n,[a] Zn^{II} Complex Formation Constants $K(ZnL)$,[b] and Deprotonation Constants (pK_a) of Zn^{II}-Bound H_2O for **1** and **3** at 25 °C

	1[c]	3[d]
log K_1	10.7	10.32 ± 0.05
log K_2	9.7	7.78 ± 0.02
log K_3	<2	4.44 ± 0.02 (4.4 ± 0.1)[e]
log K_4	<2	<2
log K_5		<2
log $K(ZnL)$	16.2	10.6 ± 0.2
pK_a (for $LZn{-}OH_2$)	7.88[f]	7.46 ± 0.02

[a] $K_n = [H_nL]/([H_{n-1}L]a_{H^+})$. [b] $K(ZnL) = [ZnL]/([Zn][L])$. [c] From ref 20 at 25 °C and $I = 0.2$ ($NaClO_4$). [d] At $I = 0.10$ ($NaNO_3$). [e] The value in parentheses was determined spectrophotometrically, see the text. [f] From ref 9. The previously reported value of 8.02 ± 0.03 (see ref 10a) was determined by potentiometric pH titration in the presence of 4 equiv of Cl^- anion. Quantitative details of the interaction of **2** with Cl^- will be reported elsewhere.

nm ($\epsilon = 3.08 \times 10^4$ for the protonated form at pH 2.5 and 1.90×10^4 for the neutral form at pH 6.9), 346 nm ($\epsilon = 1.61 \times 10^4$ and 1.26×10^4, respectively), 410 nm ($\epsilon = 7.63 \times 10^3$ and 2.05×10^3, respectively), and 431 nm ($\epsilon = 4.96 \times 10^3$ and ~0, respectively) at 25 °C and $I = 0.10$ ($NaNO_3$). The remaining values were assigned to the macrocyclic tetraamine moiety. Log K_2 for **3** (7.78 ± 0.02) is smaller than that for **1** (9.7)[20] due not to the mono N-alkylation but rather to a more hydrophobic environment or a smaller degree of solvation around the macrocycle.[21]

Synthesis and Complexation Constants of Acridine-Pendant Zn^{II}–Cyclen Complex 4·2ClO₄. The equilibrium constant for **3** and Zn^{II} was determined by pH titration of the completely protonated ligand $3{\cdot}5H^+$ (1 mM) in the presence of an equimolar amount of Zn^{II} (Figure 1b) at 25 °C and $I = 0.10$ ($NaNO_3$). The smooth buffer curve ($\sim 3 < a < 5$) indicates neutralization of the protonated cyclen and acridine accompanied by Zn^{II} complexation, until the occurrence of a break at $a = 5$ followed by the deprotonation of Zn^{II}-bound water, **4** ⇌ **8**, ($pK_a = 7.46 \pm 0.02$) at $5 < a < 6$ (Scheme 3). The strong acidity of Zn^{II} in **2** ($pK_a = 7.88$) is thus further enhanced in **4**. This can be explained by the weakened interaction between Zn^{II} and the tertiary nitrogen N(1).[22] A longer Zn^{II}–N(1) distance (hence weaker bonding) is proven by the X-ray crystal structure of the ternary complex of **4** with 1-methylthymine as described below. The 1:1 Zn^{II} complex **4** is most likely to possess a square-pyramidal configuration as found for **2**.[9]

(21) For *N*-methylcyclen, log $K_2 = 9.7$. Unpublished results.

(22) The pK_a of the water bound to Zn^{II} in the *N*-methylcyclen–Zn^{II} complex is 7.68 ± 0.02.

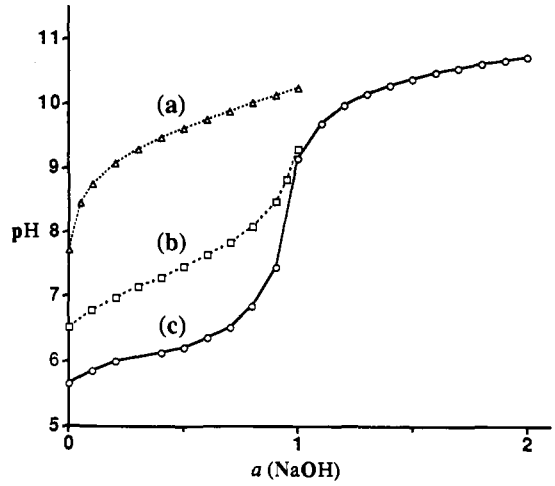

Figure 2. pH Titration data for acridine-pendant Zn^{II}–cyclen **4**·2ClO₄ at 25 °C and $I = 0.10$ ($NaNO_3$): (a) 1.0 mM dT; (b) 1.0 mM **4**·2ClO₄; (c) 1.0 mM **4**·2ClO₄ + 1.0 mM dT. a is the number of equivalents of base added.

Scheme 3

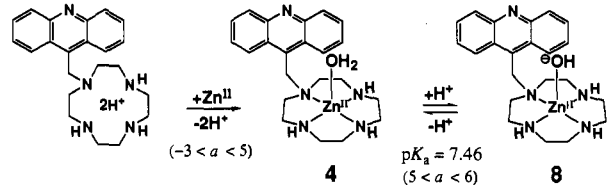

From the analysis of the titration data, the Zn^{II} complexation constant for **3**, log $K(ZnL) = (10.6 \pm 0.2)$ ($K(ZnL) = [ZnL]/([Zn][L]), M^{-1}$), was determined (Table 1). In the computation, an imaginary pK_a value of 4.5 for the acridine moiety[23] was used as the optimum for the determination of log $K(ZnL)$ and log $K(ZnHL)$ (= 4.9, $K(ZnHL) = [ZnHL]/([Zn][HL])$, M^{-1}, where HL represents the monoprotonated ligand). The log $K(ZnL)$ value for **4** is considerably smaller than that for pendantless cyclen complex **2** (log $K(ZnL) = 16.2$).[20] This may be attributed to the hydrophobic environment around the $Zn^{II}{-}OH_2$ of **4** due to the aromatic pendant as well as the weaker interaction between Zn^{II} and the tertiary N(1).

From a solution of **3** and an equimolar amount of $Zn^{II}(ClO_4)_2{\cdot}6H_2O$ in C_2H_5OH, yellowish crystals of **4**·2ClO₄ were obtained in almost quantitative yield. This compound was characterized by ^1H and ^{13}C NMR, and elemental analysis (C, H, N). A study of the interaction between **4** and several nucleosides was conducted on this complex.

Determination of Affinities of 4 for dT and Its Homologues. In order to study the interaction between acridine-pendant Zn^{II}–cyclen complex **4** and the "imide" functionality of nucleobases in aqueous solution, potentiometric pH titrations of **4** (1.0 mM) were conducted in the presence of an equimolar amount of dT and its homologues, AZT, U, Ino, BU (5-bromouridine), Ff (ftorafur), and AU (6-azauridine) at 25 °C and $I = 0.10$ ($NaNO_3$). Typical pH titration data of **4** (1.0 mM) in the absence and the presence of dT (1.0 mM) are plotted in Figure 2, parts b and c, respectively. For each thymidine homologue tested, the buffer pH region ($0 < a < 1$, corresponding to the deprotonation of the Zn^{II}-bound H_2O) significantly dropped, indicating the concomitant "imide" deprotonation upon complexation. Notably, with dT, the ternary complexation is practically completed at physiological pH (see Figure 2c).

(23) Since the neutralization of the protonated acridine nitrogen simultaneously occurs with Zn^{II} complexation with **3**, the exact deprotonation constant for the acridine nitrogen was not obtained. However, the value of 4.5 for the acridine nitrogen was found to be the optimum for the computation, which is the same as the apparent pK_a value of 4.5 ± 0.2 determined by UV spectral changes of **4** at pH 3~9.

Scheme 4

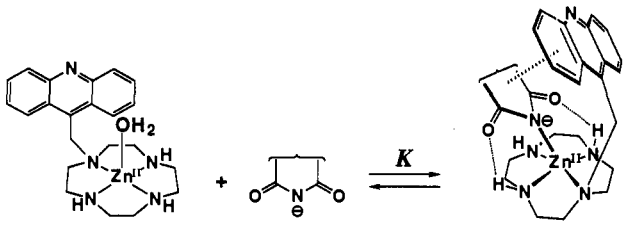

4 (ZnL) + (S) ⇌ 9 (ZnL-S)

Table 2. Comparison of pK_a Values for Deprotonation of the "Imide" or "Amide" NH's of Nucleosides and Complexation Constants, log K(ZnL–S) [L = **1** or **3**, S = N(3)- (or N(1)- for Ino) Deprotonated Nucleosides], for **2** and **4**

substrate[a]	pK_a[b]	log K(ZnL–S)[c]	
		2[d]	**4**[e]
dT	9.71 ± 0.02	5.6 ± 0.1	7.2 ± 0.1
AZT	9.67 ± 0.02	5.6 ± 0.1	7.2 ± 0.1
U	9.23 ± 0.02	5.2 ± 0.1	6.9 ± 0.1
Ino	8.75 ± 0.02	4.2 ± 0.1	5.7 ± 0.1
BU	7.97 ± 0.02		7.0 ± 0.1
Ff	7.79 ± 0.02	4.6 ± 0.1	6.6 ± 0.1
AU	6.60 ± 0.02		6.3 ± 0.1

[a] For abbreviations and structures, see Chart 2. [b] At 25 °C and I = 0.10 ($NaNO_3$). [c] Determined by a potentiometric pH titration. K(ZnL–S) is defined as [ZnL–S]/([ZnL][S]), M^{-1}. [d] From ref 9. At 25 °C and I = 0.10 ($NaClO_4$). [e] At 25 °C and I = 0.10 ($NaNO_3$). In the pH titration at I = 0.10 ($NaClO_4$) precipitation occurs.

A computation of the titration curves[9] was used to determine the equilibrium (Scheme 4) for complex **9** formation K(ZnL–S) (= [ZnL–S]/([ZnL][S])), M^{-1}, where S represents the "imide" or "amide" N-deprotonated (anionic) nucleoside. This analytical method was applied to all the nucleosides that underwent interaction with **4** with concomitant deprotonation from the N(3) (or N(1) for Ino) site. All the results are summarized in Table 2 and are compared with those for complex **2**.

An attempt was made to determine the complexation constants of **4** with dT and its homologues independently by measuring UV spectral changes of the nucleosides around 260 nm as done before with **2**.[9] However, the UV absorption bands of each guest were concealed behind those for the acridine in **4**.

The open site of **4** is available for an incoming substrate, and the three NH groups of the cyclen ring and the acridine plane are spatially directed toward it. It seemed reasonable to us to expect that, if dT or its homologues coordinated to Zn^{II} at the deprotonated N(3), the two contiguous exocyclic carbonyl oxygens would supplement the interaction by forming two hydrogen bonds with the two NH groups of the cyclen, and additionally the acridine ring would reinforce the complex stability by means of a stacking interaction with the pyrimidine ring.

In fact, the complexation constants with **4** were all found to be greater than those with **2**, supporting our prediction of an additional binding force from a stacking interaction. Among the "imide"-containing bases, the affinity order dT (log K = 7.2), AZT (7.2) > BU (7.0) > U (6.9) > Ff (6.6) > AU (6.3) is consistent with the order of the basicities of the conjugate base $N(3)^-$. Moreover, a linear relationship exists between the log K(ZnL–S) and pK_a values of the conjugate acid as depicted in Figure 3a. This fact indicates that **4** binds to all these nucleosides in the same manner with the Zn^{II}–N^- coordinate interaction acting as the controlling force. Exactly the same trend was found for **2**.[9]

The affinity trends for **4** and **2** are compared in Figure 3. Firstly, the line (a) for **4** is above the line (b) for **2**, which indicates that the acridine moiety in **4** enhances the complex stability. The stability enhanced by $\Delta\log K$ of 1.6 ~ 2.0, translated into $\Delta\Delta G°$ = 2.2 ~ 2.7 kcal/mol, is similar to the reported value of ~2.4 kcal/mol for the π–π interaction between adenine and anthracene in aqueous solution.[4c] Secondly, these two linear plots are not parallel, which implies that the stability enhancement by the acridine ring varies with each pyrimidine structure. From the shallower slope for **4**, it may be considered that the nucleobases that have the more acidic "imide" group tend to enjoy more of a stabilizing contribution from the additional stacking interaction with the acridine. The electron-withdrawing substituent on BU or Ff decreases the thymine π-electron density, which may help to increase the π–π electronic interaction.[3a,24]

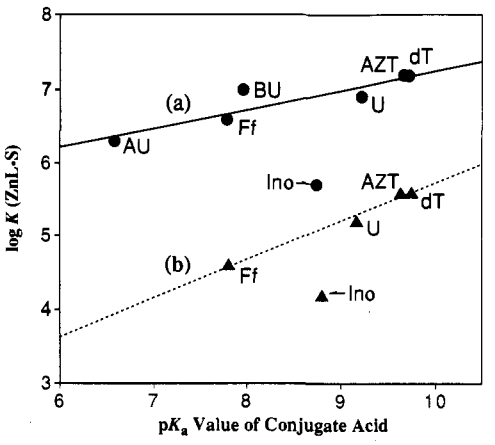

Figure 3. Plot of the complex formation constants of **2** (from ref 9) and **4** at 25 °C for N(3)- (or N(1)- for Ino) deprotonated nucleosides, log K(ZnL–S), against pK_a values for the conjugate acid: (a) ● represents **4** at I = 0.10 ($NaNO_3$); (b) ▲ represents **2** at I = 0.10 ($NaClO_4$).

As for Ino, which lacks one carbonyl group at the C(2) position of dT (see Chart 2), the affinity with **4** is smaller (log K = 5.7) than that predicted from the amide pK_a value of 8.75, as found with **2** (Figure 3). This fact again supports the notion that direct and/or indirect hydrogen bonding by the two exocyclic carbonyl groups of the thymidine derivatives serves to supplement the thermodynamic stability of the ternary complexes in aqueous solution (Scheme 5).

NMR Studies of dT in the Presence of 4. (1) Further Evidence for a Stacking Interaction. ^1H NMR studies give further proof for a stacking interaction between the acridine moiety of **4** and the pyrimidine ring of dT as well as for hydrogen bonding between the two carbonyl groups of dT and the cyclen NH groups. The ^1H NMR of a 5 mM solution of dT in the presence of an equimolar amount of **4** at 25 °C and pD 9.0 in D_2O exhibited significant upfield shifts of the methyl (at C(5)) and the adjacent vinylic (at C(6)) protons of the thymine base, the anomeric proton (1′-H) of the sugar moiety, and the aromatic protons of the acridine moiety of **4** (Table 3 and Figure 4). The 6-H and 5-Me signals of thymine base were shifted upfield by 0.42 and 0.38 ppm, respectively. The anomeric 1′-H signal was shifted upfield by a similar amount (0.67 ppm), but no significant shifts were found for the other protons of the ribose unit. The selective upfield shifts of the substrate protons are consistent with the close approach of the acridine to the substrate and its participation in binding. In contrast, with unsubstituted Zn^{II}–cyclen complex **2**, no significant shifts were found for the dT protons upon complexation (Table 3). Small upfield shifts in the range 0.12–0.26 ppm were also observed for the aromatic protons of the acridine ring, which probably arise from the face-to-face stacking interaction between the acridine moiety and the thymine base.

(2) Evidence for Hydrogen Bonding. Figure 5 shows the ^1H NMR spectral changes of a 5 mM solution of **4** with an equimolar amount of dT at 40 °C and pD 9.6 in D_2O. Two of the three NH

(24) For an experimental and theoretical estimation of π–π stacking energy and the contribution of individual intermolecular interactions, see: Hunter, C. A.; Sanders, J. K. M. *J. Am. Chem. Soc.* **1990**, *112*, 5525.

Table 3. ^{1}H NMR Chemical Shifts (δ in ppm)[a] of 4·2ClO$_4$ in the Absence and Presence of an Equimolar Amount of dT in D_2O, 5 mM, at 25 °C and pD 9.0

	acridine moiety				thymine and anomeric protons		
	4′-H	1′-H	3′-H	2′-H	6-H	1′-H	5-Me
dT[b]					7.50	6.34	1.87
4·2ClO$_4$	8.12	7.96	7.83	7.61			
dT + 4·2ClO$_4$	7.86	7.81	7.68	7.49	7.08	5.67	1.49
dT + 2·2ClO$_4$					7.52	6.32	1.87

[a] The numbering system is as follows:

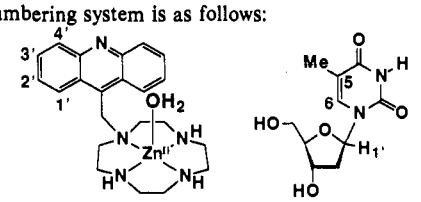

4 dT

[b] pD > 12. dT is in the N(3)-deprotonated anionic form.

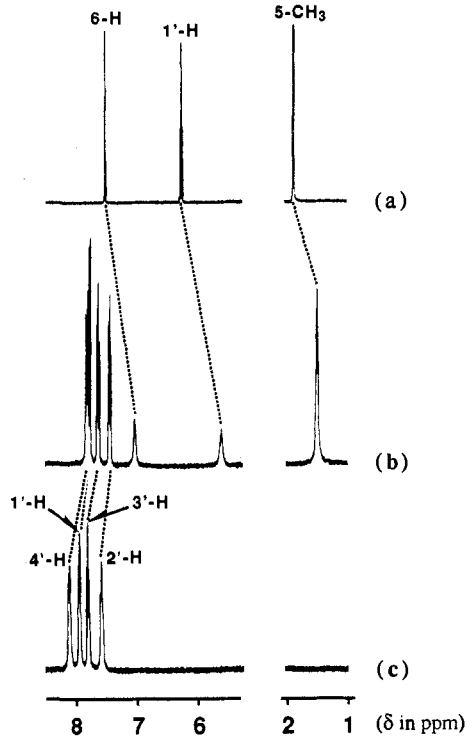

Figure 4. ^{1}H NMR spectra of (a) dT (5 mM), (b) dT (5 mM) + 4·2ClO$_4$ (5 mM), and (c) 4·2ClO$_4$ (5 mM) at 25 °C and pD 9.0.

protons of the cyclen subunit in this complex shown as a broad peak at ~3.57 ppm exchanged very slowly with deuterium, and this signal disappeared only after about 70 h. However, the deuterium-exchange reaction for **4** or the ternary complex of **2** with dT was more rapid and was complete within 24 h or a few hours, respectively (still slower than that for **2** in the absence of dT), at 25 °C. These observations are best explained by the (direct and/or indirect) hydrogen bonding between the two carbonyl oxygens of dT and the cyclen NH groups of **4** being stabilized by the hydrophobic environment. In particular, the hydrogen bonds formed in **4** are presumed to be less flexible and thus more stationary compared to those in **2**,[9] because the guest dT is fixed parallel to the plane of the acridine ring.

Unequivocal Evidence for the "Multipoint" Recognition. X-ray Crystal Structure of the Ternary Complex of 4 with N(3)-Deprotonated 1-Methylthymine 10·ClO$_4$·2H$_2$O. Fortunately, we could isolate a new ternary complex between **4** and N(3)-deprotonated 1-methylthymine. From a mixture of equimolar amounts of 1-methylthymine, 4·2ClO$_4$, and NaOH in CH_3CN–H_2O, pale yellow prisms precipitated (Scheme 5) which were found to be suitable for X-ray analysis after recrystallization from CH_3OH–H_2O. The elemental analysis (C, H, N) fits to a 1:1 ternary complex **10** with a monoanion ClO_4^- and two water molecules, implying that the other anion is located at the deprotonated thymine N(3).

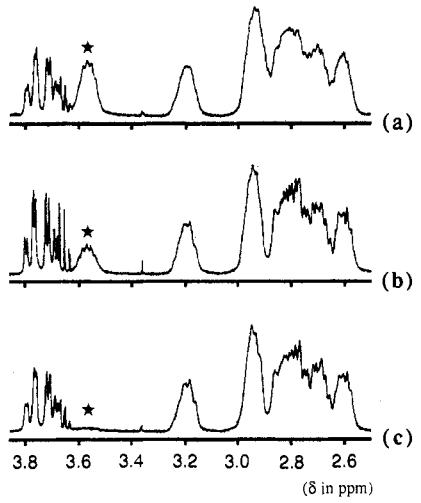

Figure 5. ^{1}H NMR spectral change of D-exchangable amine protons in 4·2ClO$_4$ in the presence of an equimolar amount of dT in D_2O (5 mM) at 40 °C and pD 9.6 (a) immediately after mixing, (b) 10 h after mixing, and (c) 70 h after mixing.

Scheme 5

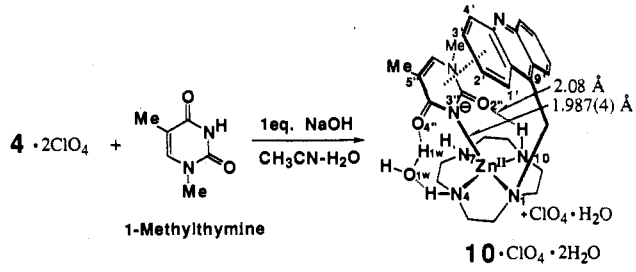

Further evidence for the structure of the imide N(3)-deprotonated complex **10** comes from the lowered C=O stretching frequencies (KBr pellet, $\nu_{C=O}$) from 1699 cm^{-1} for 1-methylthymine to 1661 and 1626 cm^{-1} for **10**·ClO$_4$·2H$_2$O (Table 4), reflecting the longer conjugation of the carbonyls due to the deprotonation of the N(3)–H group.

Figure 6 shows the ORTEP drawing of **10** with 50% probability thermal ellipsoids. Crystal data and data collection parameters are displayed in Table 4. Selected bond distances, interligand distances, and bond angles are listed in Table 5. The ternary complex **10** assumes a distorted square-pyramidal structure with coordination from four nitrogens (N(1), N(4), N(7), and N(10)) of the cyclen moiety and an N(3″)-deprotonated imide anion of the pyrimidine ring. The most remarkable feature of the coordinate structure is the very short Zn(1)–N(3″) bond distance of 1.987(4) Å (cf. 2.053(8) Å in **6**).[9] This fact is in agreement with our earlier findings that the strongly acidic Zn^{II} in macrocyclic complexes prefers N^- anion donors over neutral nitrogen donors.[10,15,25] The distance between Zn(1) and the tertiary N(1) (2.362(4) Å) is longer (and thus weaker) than those between Zn^{II} and each secondary NH group (Zn(1)–N(4, 7, or 10), the average is 2.121(4) Å), which may be offset by the shortest (thus strongest) Zn(1)–N(3″) bond.

All three NH groups of the cyclen ring are spatially directed toward the thymine base bound to the central Zn^{II} ion. The

(25) Kimura, E.; Koike, T. *Comments Inorg. Chem.* **1991**, *11*, 285.

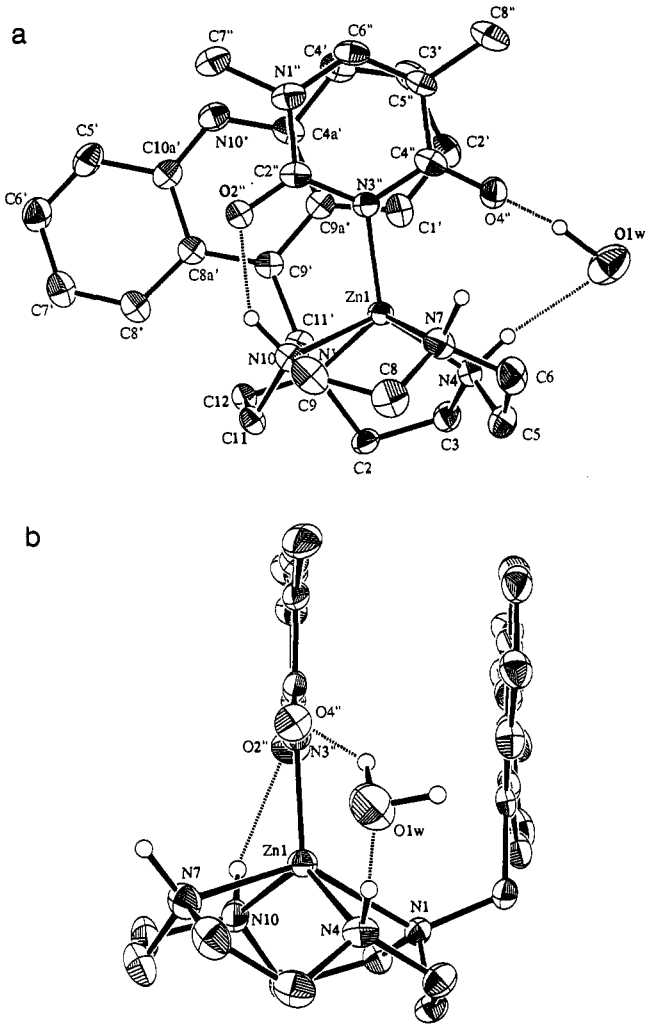

Figure 6. ORTEP drawing (50% probability ellipsoids) of **10**·ClO_4·$2H_2O$: (a) perpendicular to and (b) in the plane of the acridine moiety. A perchlorate anion and one of the two water molecules are omitted for clarity.

Table 4. Crystallographic Parameters of **10**·ClO_4·$2H_2O$

formula	$C_{28}H_{40}N_7O_8Cl_1Zn_1$
fw	703.50
cryst color, habit	pale yellow, prismatic
cryst dimens, mm	0.40 × 0.20 × 0.10
cryst system	monoclinic
space group	$C2/c$ (#15)
lattice type	C-centered
lattice params	a = 15.312(3) Å
	b = 21.920(3) Å
	c = 18.774(2) Å
	β = 101.68(1)°
	V = 6171(1) Å^3
Z	8
ρ_c, g cm^{-3}	1.515
radiation	Cu Kα (λ = 1.541 78 Å)
μ, cm^{-1}	24.27
$2\theta_{max}$, deg	120.1
refinement	full-matrix least-squares method
no. of measd reflcns	4943
no. of indep reflcns ($\|I_0\| > 3\sigma(I_0)$)	3573
R	0.062
R_w	0.093

carbonyl oxygen O(2″) of the pyrimidine ring forms a hydrogen bond directly with a cyclen N(10)–H group (O(2″)–N(10), 2.881(5) Å; O(2″)- - -H(10)–N(10), 137°), while the other carbonyl oxygen O(4″) binds indirectly via a water molecule with a diagonal N(4)–H group (O(4″)- - -O(1_w) = 2.731(6) Å, O(4″)- - -H(1_w)–O(1_w) = 143°, N(4)- - -O(1_w) = 3.154(7) Å, N(4)–H(4)- - -O(1_w) = 169°) (Figure 6a).

Table 5. Selected Bond Distances (Å), Interligand Distances (Å), and Bond Angles (deg) of **10**·ClO_4·$2H_2O$[a]

Zn(1)–N(3″)	1.987(4)	Zn(1)–N(1)	2.362(4)
Zn(1)–N(4)	2.099(4)	Zn(1)–N(7)	2.181(4)
Zn(1)–N(10)	2.084(4)	O(2″)–C(2″)	1.235(6)
O(4″)–C(4″)	1.236(6)	N(3″)–C(2″)	1.361(6)
N(3″)–C(4″)	1.379(6)		
N(3″)–Zn(1)–N(1)	113.8(1)	N(3″)–Zn(1)–N(4)	127.5(2)
N(3″)–Zn(1)–N(7)	106.8(2)	N(3″)–Zn(1)–N(10)	105.2(2)
N(1)–Zn(1)–N(4)	80.1(1)	N(1)–Zn(1)–N(7)	138.4(1)
hydrogen bond			
O(2″)---N(10)	2.881(5)	O(4″)---O(1_w)	2.731(6)
N(10)–H(10)	0.98	O(1_w)–H(1_w)	1.12
O(2″)---H(10)	2.08	O(4″)---H(1_w)	1.75
O(2″)---H(10)–N(10)	137	O(4″)---H(1_w)–O(1_w)	143
		N(4)---O(1_w)	3.154(7)
		N(4)–H(4)	0.94
		O(1_w)---H(4)	2.22
		N(4)–H(4)---O(1_w)	169
stacking			
N(1″)---C(4a′)	3.398(8)	N(1″)---N(10′)	3.590(6)
C(2″)---C(9a′)	3.370(3)	C(2″)---C(4a′)	3.456(5)
O(2″)---C(9′)	3.468(3)	O(2″)---C(8a′)	3.524(6)
N(3″)---C(1′)	3.355(4)	N(3″)---C(9a′)	3.373(4)
C(4″)---C(1′)	3.459(3)	C(4″)---C(2′)	3.440(4)
C(5″)--C(2′)	3.591(3)	C(5″)---C(3′)	3.424(4)
C(6″)---C(4′)	3.415(6)	C(7″)---N(10′)	3.473(3)

[a] ESD in parentheses.

Figure 6b shows the crystal structure viewed approximately parallel to the plane of the thymine base and the acridine ring with the dihedral angle of 2.5°. The acridine moiety lies face-to-face with the plane of the thymine substrate with the interplane separation ranging from 3.285 to 3.419 Å (normally ~3.4 Å for a cofacial interaction).[24,26] Both views in Figure 6 depict a well-arranged interfacial stacking between the acridine at C(1′), C(2′), C(4′), C(4a′), and C(9a′) and the pyrimidine ring. The overlapped positions of the acridine and the pyrimidine ring account for the aforementioned ^{1}H NMR upfield shifts of protons on the periphery of the thymine base and the absence of any shifts for the ribose protons further away from the acridine ring current.

More significantly, the position of the N(3″) of the 1-methylthymine is distorted away from the regular apex position of a square pyramid so that the thymine ring is ideally situated for stacking with the acridine ring (N(3″)–Zn(1)–N(1) = 113.8(1)° > N(3″)–Zn(1)–N(7) = 106.8(2)°), as well as to make the carbonyl oxygen O(2″) form a direct hydrogen bond with the cyclen N(10)–H [(N(3″)–Zn(1)–N(10) = 105.2(2)° < N(3″)–Zn(1)–N(4) = 127.5(2)°]. The other carbonyl oxygen O(4″) is linked with the cyclen N(4)–H via a water molecule (Scheme 6a). However these distortions are thermodynamically compensated by the energy gain from the π–π stacking and hydrogen bonding. For comparison, in **6** without the acridine functionality, a more ideal square-pyramid coordinate structure was observed (Scheme 6b).[9]

A lattice picture of the complex **10**·ClO_4·$2H_2O$ drawn down the b crystallographic direction is illustrated in Figure 7 and shows an assembly with a regular stacking array. In the complex **10**·ClO_4·$2H_2O$, an intermolecular stacking occurs, which involves a sequence of intermolecular stacked pairs of thymine (T) and acridine (Acr) subunits in the order of –T–T–Acr–Acr–. The intramolecular distance between Acr and Acr, or T and T, is within 3.3~3.4 Å, which is consistent with a strong cofacial stacking interaction.

Interaction between 4 and Other Nucleosides, dA, dC, and dG. With dA and dC (both contain no dissociable NH), the pH

(26) Saenger, W. *Principles of Nucleic Acid Structure*; Springer-Verlag: New York, 1984; pp 132.

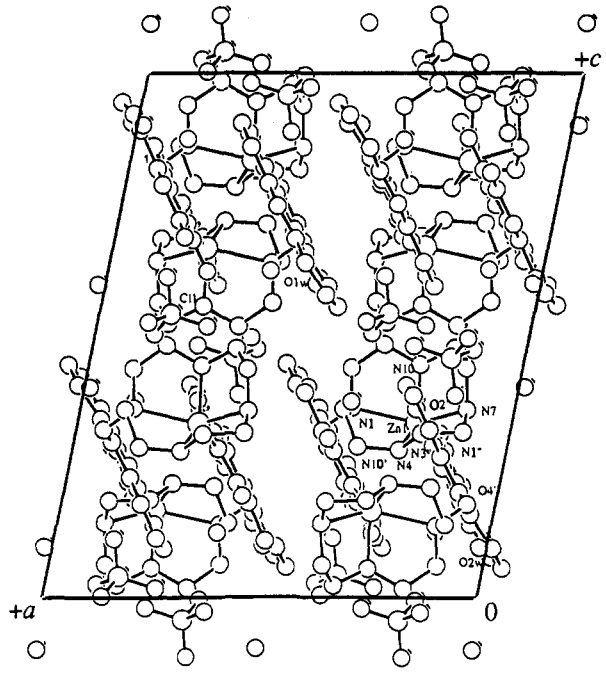

Figure 7. Lattice picture of the complex **10**·ClO_4·$2H_2O$ drawn down the *b* crystallographic direction.

Scheme 6

(a)

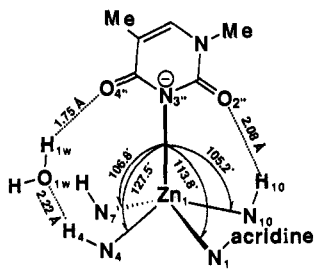

10

(b)

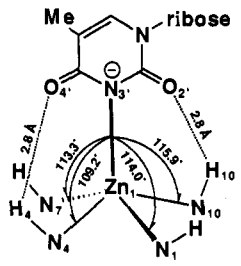

6 (AZT-2 complex)

titration curves of **4** did not change at all, just as found with **2**.[9] This result indicates that no functionality on the periphery of dA and dC interacts with the Zn^{II} in **4** although the purine or pyrimidine ring may possibly interact with the acridine moiety.

On the other hand, **4** interacts with dG whereas **2** does not bind to dG at all.[9] The pH titration data of **4** (1.0 mM) in the absence and the presence of dG (1.0 mM) are plotted in Figure 8. This shows that, compared with the dT homologues, the interaction between **4** and dG is quite different and much weaker. For instance, the buffer pH region of **4** ($0 < a < 1$, corresponding to the deprotonation of the Zn^{II}-bound H_2O) is significantly raised (Figure 8c), which indicates that the uncharged exocyclic amino group at C(2), the carbonyl group at C(6), or the aromatic nitrogen N(7) in dG binds to Zn^{II} in **4** and not the N(1)-deprotonated "imide" nitrogen. From the detailed analysis of the titration

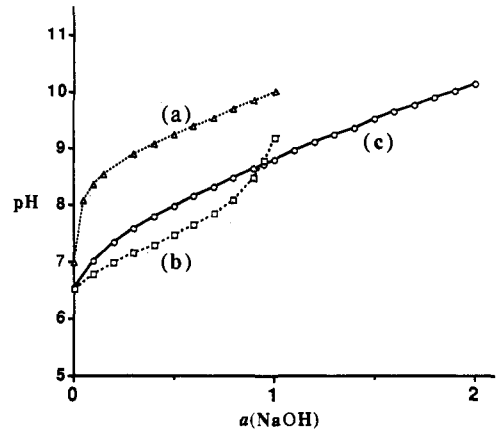

Figure 8. pH Titration data for acridine-pendant Zn^{II}–cyclen **4**·$2ClO_4$ at 25 °C and $I = 0.10$ ($NaNO_3$): (a) 1.0 mM dG; (b) 1.0 mM **4**·$2ClO_4$; (c) 1.0 mM **4**·$2ClO_4$ + 1.0 mM dG. *a* is the number of equivalents of base added.

Scheme 7

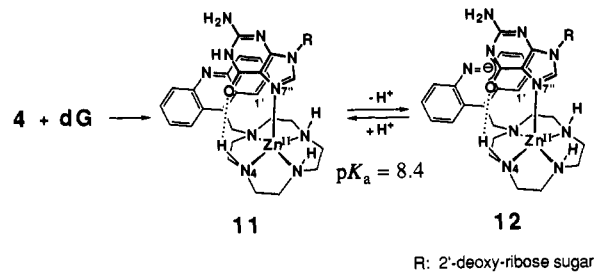

curve ($0 < a < 2$) (for the computation, see the Experimental Section), the mode of complexation of **4** with dG can be postulated as depicted in Scheme 7 (the atom numbering follows that used in Figure 9). The structure of the 1:1 ternary complex of **4** with the free form of dG, **11**, was firmly proven by X-ray analysis as described below. From the pH titration data, the complexation constants, $\log K = 4.1 \pm 0.1$ for the free form and $\log K = 5.0 \pm 0.1$ for the N(1″)-deprotonated form of dG, and the "amide" pK_a value of 8.4 for dG in **11** were obtained. The increase in acidity of the "amide" N(1″)–H compared to uncomplexed dG ($pK_a = 9.27 \pm 0.02$) may be due to a hydrogen bond between the carbonyl oxygen O(6″) of dG and the cyclen N(4)–H group. Thus **4** interacts with dG in quite a different manner. However, **4** is still selective for dT at physiological pH. For instance, in a mixture of dT (1 mM) and dG (1 mM) in the presence of 1 mM of **4** at pH 7.6 and 25 °C, 71% of **4** forms a ternary complex with N(3)-deprotonated dT while only 24% complexes dG (21% for the free form **11** and 3% for the deprotonated form **12**).[27]

The ^{13}C NMR of a dimethyl sulfoxide-d_6 solution of **11**, upon addition of 1 molar equiv of NaOD (where the N(1)-deprotonated 1:1 ternary complex **12** is formed), exhibited 4 ~ 11 ppm downfield shifts for C(2″), C(4″), and C(5″) due to the "amide" deprotonation of dG. In contrast, only a slight upfield shift (2 ppm) was found for C(8″). Similar results were observed with uncomplexed dG. It is highly likely that the binding mode does not change at the N(7″) site (see **12**) upon deprotonation. This is not entirely unexpected since complementary hydrogen bonding is still possible at this site and steric crowding would preclude binding at the N(1)-deprotonated site.

X-ray Crystal Structure of a Ternary Complex 11 Composed of 4 and dG. From a mixture of equimolar amounts of dG and **4**·$2ClO_4$ in CH_3CN–H_2O, orange prisms precipitated which were suitable for X-ray analysis. The elemental analysis (C, H, N) fits to a 1:1 ternary complex **11** containing two BF_4^- anions and

(27) At pH 8.4, 83% of **4** forms a ternary complex with dT while 14% complexes dG (where [**11**] = [**12**]).

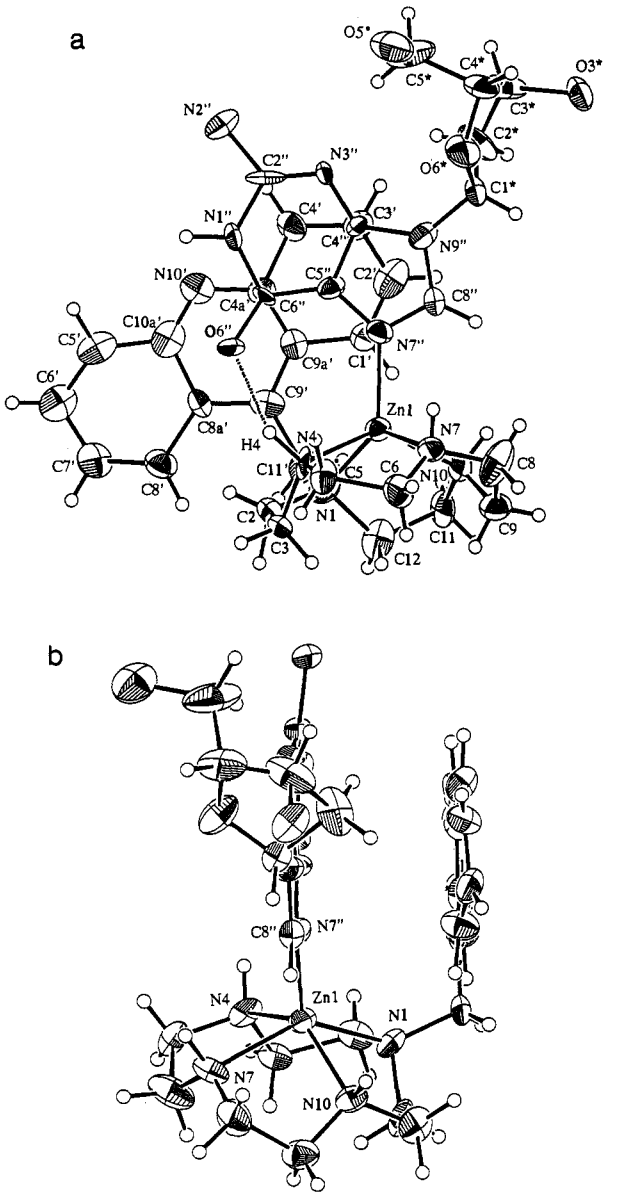

Figure 9. ORTEP drawing (30% probability ellipsoids) of **11**·2BF_4·2.5H_2O: (a) perpendicular to and (b) in the plane of the acridine moiety. Two tetrafluoroborate anions and water molecules are omitted for clarity.

two and one-half water molecules, which implies that the "amide" proton at N(1″) is not deprotonated. Further evidence for the free form of dG in **11** comes from the unaltered C=O stretching frequencies (KBr pellet, $\nu_{C=O}$) of 1694 cm^{-1} (cf. 1692 cm^{-1} for dG itself in the free form).

Figure 9 shows the ORTEP drawing of **11** with 30% probability thermal ellipsoids. Crystal data and data collection parameters are displayed in Table 6. Selected bond distances, interligand distances, and bond angles are listed in Table 7. Two crystallographically independent **11** molecules, four BF_4^- anions, and five water molecules are included in an asymmetric unit. The complexes have very similar conformations, excluding those of the $-CH_2OH$ groups of sugar moieties. Since the BF_4^- ions are suggested to be disordered (R = 0.083 and R_w = 0.104) by inspection of a difference electron density map and no disordered model can definitely be located, we are unable to discuss the structure of **11** in detail. However, it undoubtedly shows a distorted square-pyramidal Zn–N_5-coordinate structure with four nitrogens (N(1), N(4), N(7), and N(10)) of the cyclen moiety and an N(7″) of the purine ring. The distance between Zn(1) and N(7″) is 2.04(1) Å and is slightly longer than that between

Table 6. Crystallographic Parameters of **11**·2BF_4·2.5H_2O

formula	$C_{32}H_{47}N_{10}O_{6.5}B_2F_8Zn_1$
fw	914.77
cryst color, habit	orange, prismatic
cryst dimens, mm	0.30 × 0.25 × 0.10
cryst system	monoclinic
space group	$P2_1$ (#4)
lattice type	primitive
lattice params	a = 10.892(4) Å
	b = 21.230(2) Å
	c = 17.465(2) Å
	β = 100.19(1)°
	V = 3974(1) Å^3
Z	4
ρ_c, g cm^{-3}	1.530
radiation	Cu Kα (λ = 1.541 78 Å)
μ, cm^{-1}	17.09
$2\theta_{max}$, deg	120.1
refinement	full-matrix least-squares method
no. of measd reflcns	6491
no. of indep reflcns ($\|I_0\| > 3\sigma(I_0)$)	4473
R	0.083
R_w	0.104

Table 7. Selected Bond Distances (Å), Interligand Distances (Å), and Bond Angles (deg) of **11**·2BF_4·2.5H_2O[a]

Zn(1)–N(7″)	2.04(1)	Zn(1)–N(1)	2.36(1)
Zn(1)–N(4)	2.01(1)	Zn(1)–N(7)	2.16(1)
Zn(1)–N(10)	2.09(1)	O(6″)–C(6″)	1.26(1)
N(7″)–Zn(1)–N(1)	123.3(5)	N(7″)–Zn(1)–N(4)	109.1(5)
N(7″)–Zn(1)–N(7)	98.6(4)	N(7″)–Zn(1)–N(10)	112.9(5)
N(1)–Zn(1)–N(4)	83.0(5)	N(1)–Zn(1)–N(7)	138.1(5)
hydrogen bond			
O(6″)---N(4)	3.01(1)	N(4)–H(4)	0.94
O(6″)---H(4)	2.20		
stacking			
N(1″)–C(4a)	3.39(2)	N(1″)---C(4′a)	3.28(2)
N(1″)---N(10′)	3.28(2)	C(2″)---C(4′)	3.37(2)
N(3″)---C(4′)	3.58(2)	C(4″)---C(3′)	3.38(2)
C(5″)---C(1′)	3.39(2)	C(5″)---C(2′)	3.60(2)
C(5″)---C(4′a)	3.44(2)	C(5″)---C(9′a)	3.44(2)
C(6″)---C(4′a)	3.12(2)	C(6″)---C(9′a)	3.35(2)
C(6″)---N(10′)	3.40(2)		

[a] ESD in parentheses.

Zn(1) and the anionic nitrogen N(3″) (1.987(4) Å) in **10**. The distance between Zn(1) and the tertiary N(1) (2.36(1) Å) is longer (and therefore weaker) than those between Zn^{II} and each secondary NH group (Zn(1)–N(4, 7, or 10), the average is 2.09(1) Å).[28]

All three NH groups of the cyclen ring are spatially directed toward the guanine base bound to the central Zn^{II} ion. The carbonyl oxygen O(6″) of the purine ring appears to form a hydrogen bond with a cyclen N(4)–H group (O(6″)–N(4) = 3.01(1) Å and O(6″)–H(4) = 2.20 Å) (Scheme 8). The above-mentioned lack of interaction between **10** and dA can be safely rationalized from the present X-ray study results in that a repulsive interaction would probably occur between the amino group at C(6) in dA and the cyclen NH groups which would block the access of the N(7) of dA to the Zn^{II} in **4**.

Figure 9b shows the crystal structure viewed approximately parallel to the plane of the guanine base and the acridine ring. A strong cofacial stacking interaction is found between the acridine

(28) It is to be noted that dG in the ternary complex **11** has a *syn* conformation as seen in dG of left-handed Z-DNA. In normal right-handed B-DNA, all of the nucleotides have an *anti* conformation (ref 26). The *syn* conformation here is brought about by rotating the purine residue about its glycosyl bond. Since the pendantless cyclen–Zn^{II} complex **2** efficiently inverts DNA helicity from the B to Z form (Shionoya, M.; Kimura, E.; Hayashida, H.; Petho, G.; Marzilli, L. G. *Surpramol. Chem.* **1993**, *2*, 173), **4** might be able to interact more strongly with the imidazole ring of dG prominent on the outer part of the Z-DNA molecule since there is considerable exposure of the guanine N(7) and C(8). We are currently testing this hypothesis.

Scheme 8

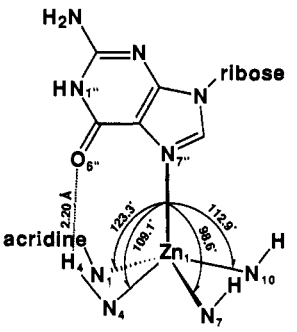

at C(1′), C(2′), C(3′), C(4′), and C(4a′) and the purine ring with the plane-to-plane separation ranging from 3.1 to 3.4 Å. Since little interaction was observed between Zn^{II} in the acridine-free cyclen complex **2** and N(7) of dG,[9] the coordination of N(7″) of dG to **4** must be assisted by the strong π–π stacking interaction. If we assume that the stacking contributes $\Delta\log K \sim 2$, as discussed above, then the coordination of N(7″) of dG to **4** should bring $\Delta\log K \sim 2$, which explains the little (i.e., unmeasurable) interaction observed between **2** and dG.

More significantly, as seen in **10**, the position of the N(7″) of dG is distorted away from the regular apex position of a square pyramid so that the guanine ring is ideally situated for stacking with the acridine ring (N(7″)–Zn(1)–N(1) = 123.3(5)° > N(7″)–Zn(1)–N(7) = 98.6(4)°), as well as to make the carbonyl oxygen O(6″) form a direct hydrogen bond with the cyclen N(4)–H [(N(7″)–Zn(1)–N(4) = 109.1(5)° < N(7″)–Zn(1)–N(10) = 112.9(5)°]. These distortions, however, are compensated by the energy gain from the π–π stacking and hydrogen bonding.

Fluorescence Studies to Measure the Nucleoside–4 Interaction. Fluorescence emission spectrophotometry was used to observe the stacking interaction between the acridine moiety of **4** and the nucleobases. **4** has UV–visible absorption at 253 nm ($\epsilon = 1.19 \times 10^5$), 346 nm ($\epsilon = 6.06 \times 10^3$), 361 nm ($\epsilon = 9.85 \times 10^3$), 374 nm ($\epsilon = 5.81 \times 10^3$), and 390 nm ($\epsilon = 4.12 \times 10^3$) in HEPES buffer (10 mM, pH 7.6, at 25 °C and I = 0.10 ($NaNO_3$)). In dilute aqueous solutions **3** and **4** are strongly fluorescent. Excitation of **3** and **4** at 361 nm produces a fluorescence emission at 438 nm and 441 nm, respectively. Fluorescence spectra of **3** and **4** (each 10 μM) in the presence (10 μM) and the absence of nucleosides (dT, Ino, dG, dA, and dC) were measured in the above buffer solution. The strong acridine fluorescence of the ligand **3**, diprotonated at pH 7.6, remained constant in the presence of the nucleosides. In contrast, a strong decay in the fluorescence intensity of **4** occurred upon the addition of dT or Ino (Figure 10). This demonstrates the importance of the Zn^{II} within **4** for an effective interaction with "imide"-deprotonated dT homologues, leading to simultaneous interaction with the acridine group. The degree of the decay was found to increase with an increase in the affinity of **4** for the nucleobase (Table 8).[29] This finding suggests that the emission is dramatically reduced due to the N(3)-deprotonated dT or the N(1)-deprotonated Ino being bound to Zn^{II}. Not only a stacking interaction but also a negative charge upon the nucleobases may enhance the degree of energy quenching.

The addition of dA and dC hardly affected the fluorescence intensity of the acridine, in accordance with a lack of interaction with **4**, as predicted from the pH titration study. A similar effect was observed only with dG, but when 1 mM dG (100-fold excess) was used (spectrum not shown), the fluorescence intensity decreased by a factor of 0.21,[30] reflecting the weaker interaction between dG and **4**. No significant change was observed with **3** under the same conditions. The origin of this quenching effect is being investigated further.

(29) Under these conditions, 27% of dT and 6% of dG form ternary complexes with **4**.

(30) AMP and CMP were found to enhance the emission of acridine derivatives whereas GMP quenched the emission through stacking interactions. See: Georghiou, S. *Photochem. Photobiol.* **1975**, *22*, 103; **1976**, *24*, 417.

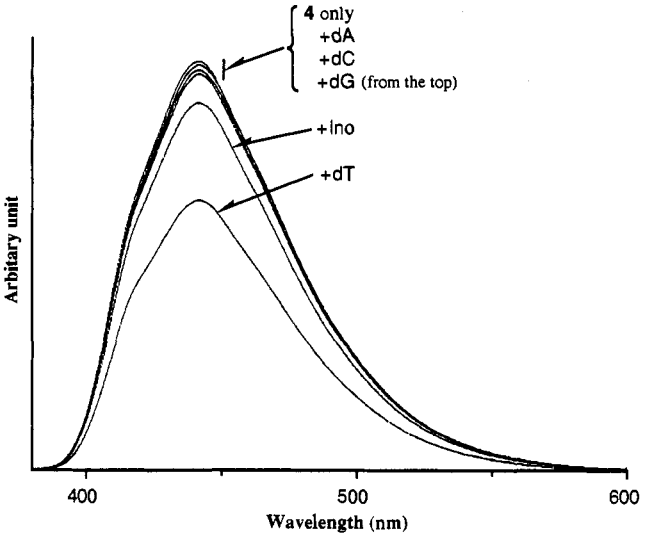

Figure 10. Fluorescence spectra of acridine-pendant Zn^{II}–cyclen **4**·2ClO_4 (10 μM) with or without nucleosides (10 μM) in HEPES buffer at 25 °C and pH 7.6 (I = 0.10 ($NaNO_3$)).

Table 8. Relative Fluorescence Intensities of **3** and **4** in the Presence of Various Nucleosides[a]

nucleoside	3	4
none	1	1
dT	0.98	0.66
Ino	0.99	0.90
dG	1	0.97
dC	0.98	0.98
dA	0.99	0.99

[a] All solutions were buffered with 10 mM HEPES buffer (pH 7.6) at 25 °C and I = 0.10 ($NaNO_3$). The concentrations of **3**, **4**, and nucleosides added were each 10 μM. Excitation was at 361 nm; emission was measured at the emission maximum centered near 438 nm for **3** and 441 nm for **4**. Errors are within ±3%.

Summary and Conclusion

The newly synthesized Zn^{II} complex of acridine-pendant cyclen **4** is a new type of artificial receptor which binds with thymidine and its homologues containing an "imide" functionality by means of a "multipoint" recognition process. The ternary complex of **4** with dT is *very stable and does not dissociate in aqueous solution at physiological pH*. The "multipoint" interaction involves a deprotonated imide–Zn^{II} bond, a π–π stacking interaction between the acridine moiety of **4** and the thymine base, and one direct and one indirect (through one water molecule) hydrogen bond between two NH groups of the cyclen ring and the two (imide) carbonyl oxygens of the thymine base. ^{1}H NMR spectra of dT in the presence of **4** in aqueous media exhibit upfield shifts for a set of thymine and anomeric sugar protons as well as for the acridine protons, which points to an appreciable π–π stacking interaction accompanying the coordination of thymine to Zn^{II}. In addition, the extremely slow deuterium exchange of two of the cyclen NH protons supports the notion of strong hydrogen bonding between the two NH groups in **4** and the two "imide" oxygens of dT. The acridine–pyrimidine π–π interaction contributes to a higher 1:1 complex stability with **4** ($\log K$ = 7.2) compared to that with the acridine-free host **2** ($\log K$ = 5.6).[9] The X-ray crystal structure of the 1:1 ternary complex **10** with 1-methylthymine is consistent with the structure concluded from the above solution behavior. The "imide"-deprotonated dT binding is responsible for the strong quenching of the fluorescence from the acridine in **4**. As for the interaction of **4** with other nucleosides, only dG interacts, but as a weaker guest with log K values of 4.1 and 5.0 for the 1:1

complexes **11** and **12**, respectively. Since the acridine-free Zn^{II}–cyclen complex **2** shows little interaction with dG, it is concluded that the acridine–purine π–π interaction greatly assists the formation of **11** and **12**. The X-ray crystal structure of **11** supports π–π stacking and Zn^{II}–N(7″) coordination. On the basis of the obtained complexation constants for **4** and these nucleosides, we estimate that **4** complexes only with dT (71%) and dG (24%) in aqueous solutions containing equivalent amounts of dT, dG, dA, and dC (each 1 mM) at pH 7.6 and 25 °C. Hence, **4** is still selective for dT at physiological pH. Further application of the new host **4** to biological systems including DNA or RNA is the subject of our current study.

Acknowledgment. We thank the Ministry of Education, Science, and Culture in Japan for the financial support of a Grant-in-Aid for Scientific Research (A) (No. 04403024) and a Grant-in-Aid for Scientific Research on Priority Areas ("Bioinorganic Chemistry") (No. 03241105). We are also grateful to the Medical Molecules Exploring Center at Hiroshima University School of Medicine.

Supplementary Material Available: Tables of atomic coordinates and equivalent isotropic temperature factors, anisotropic temperature factors, and bond distances and angles for **10**·ClO_4.$2H_2O$ and **11**·$2BF_4$·$2.5H_2O$ and listings of programs used for the binding studies (68 pages); listings of observed and calculated structure factors for **10**·ClO_4.$2H_2O$ and **11**·$2BF_4$·$2.5H_2O$ (56 pages). This material is contained in many libraries on microfiche, immediately follows this article in the microfilm version of the journal, and can be ordered from the ACS; see any current masthead page for ordering information.